

## A Behavior of Strobe Light in Non-Visibility (Dense Fog) Environments

Jai Wan Cho, Young Soo Choi, and Kyung Min Jeong

Div. Nuclear Convergence Technology Development, Korea Atomic Energy Research Institute

[jwcho@kaeri.re.kr](mailto:jwcho@kaeri.re.kr)

### 1. Introduction

In the case of a DBA (or severe accident) of the nuclear power plant accident, coolant should be injected over the reactor pressure vessel to cool the reactor core. Cold coolant that has been poured into the reactor pressure vessel would be discharged through the nozzles of the core spray system or through pipelines in the fire protection system. The discharging cold coolant would impact high temperature structures with surface temperatures of around 250°C or higher, such as the reactor pressure vessel that surrounds the reactor core, and then evaporate and turn into steam. The steam cools while forming mist (aerosol including radioactivity), which can cause a sharp drop in visibility [1].

Assuming that a robot has been deployed to manage and mitigate the DBA (or severe accident) at the nuclear power plant, the robot must perform its task in a non-visibility environment. A color CCD/CMOS camera corresponding to visible wavelength (400~700 nm) can be attached to the robot for observation and navigation. The camera needs lights in order to secure a clear field of view. Generally, the aperture of a lens is correlated to the intensity of illumination. The brighter the light, the smaller the aperture can be. If the aperture becomes narrower to the size of a pin hole, a clearer image in deep focus can be obtained. As the aperture decreases in the half, the required amount of light doubles.

In this study, a strobe light was used to understand the behavior of light in an aerosol-like non-visibility environment. Fog was injected into a vinyl pleated cylindrical fog box that is 1 m in diameter and 5.5 m in length. After the fog concentration became saturated in the fog box, the strobe light was set off at regular time intervals until the fog particles almost dissipated in the box. Images of the behavior of the light from the strobe were taken from outside of the fog box with a digital camera in line with the strobe light sync signal. The observed behavior of the strobe light was analyzed using an image processing technique.

### 2. Experiments

Figure 1 shows a block diagram of the experimental setup. A fog particles were injected into the fog box, the size of the injected fog particle were 1 to 2  $\mu\text{m}$  in diameter. The length of the rubber hose is approximately 5 m, and it has holes with a diameter of 10 mm at 50 cm intervals. The fog particles enter the

box through these holes. The fog box is composed of corrugated structure with a diameter of 1 m and approx. 5.5 m length. Both sides of the fog box were made of transparent acrylic in order to be able to see inside the box. A strobe light was placed inside the fog box.

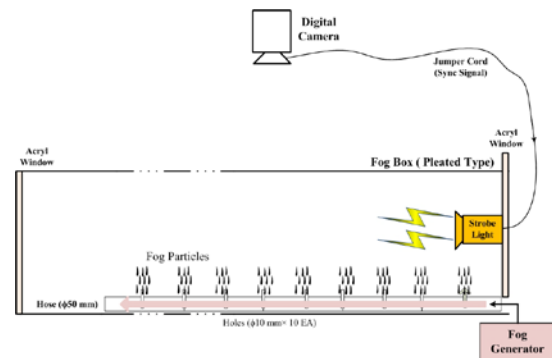


Figure 1. Block diagram of an experimental setup.

An image capture signal of the digital camera outside the fog box, as shown in Fig. 1, was coupled with the sync signal of the strobe light. The strobe light was set off at a regular time interval for about 32 min. About 8 minutes were needed to inject the fog particles into the fog box until the fog concentration was saturated in the box. After fog injection, about 24 minutes were elapsed for the concentration of the fog particles in the fog box to be dissipated nearly. The propagation shape of the strobe light inside the fog box was captured with a digital camera, placed outside of the fog box as shown in Fig. 1.

Figure 2 show propagation images of the strobe light within the fog box. The brighter area on the right-hand side in Fig. 2 shows where the strobe light was located, indicating that the light was propagating from right to left with respect to the strobe light. The shutter speed of the digital camera was 1/60s. Figure 2(b) shows an image taken 90 s after the fog started to be injected into the fog box. Figure 2(d) shows an image taken 8 minutes after injection into the box, which is the point at which the fog density is about to be saturated. In contrast to the image in Fig. 2(a) that was taken before the fog injection, the shape of the strobe light has moved toward the right (in the opposite direction from the light). The fog machine on the right-hand side is barely seen in the image before fog injection, shown in Fig. 2(a), but it is clearly seen in the images taken during fog injection (Figs. 2(c) and 2(d)). This is

because the strobe light has been reflected by fog particles.

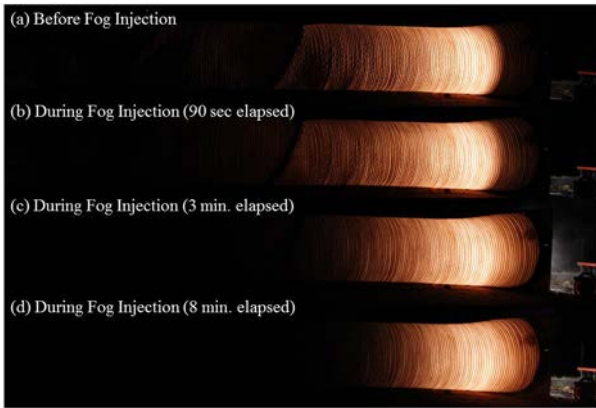


Figure 2. Observation images of the strobe light

When comparing Fig. 2(b) (an image taken after 90 s of fog injection) with Fig. 2(d) (an image taken after 8 min of fog injection when the fog density in the box has been saturated), a size of propagation shape of the strobe light was lengthened. When the fog density in the fog box was high, as shown in Fig. 2(d), the strobe light did not spread out; rather, it was trapped.

### 3. Image Processing

An image processing technique was used to analyze the propagation shape of the strobe light in the fog box according to the fog injection. At first, we used a threshold process as a pre-processing to segment the strobe light region from a background image. The threshold value for the segmentation process was properly determined using the result of image projection technique in the X-axis direction (or Y-axis direction). From the result of the segmentation process, the propagation shape (brighter region compared to the background region) of the strobe light was extracted. And a contour of the propagation shape of the strobe light was derived from the segmentation (binary) image. Then, center coordinates (X-axis and Y-axis) of the contour and a size (width and height) of the contour were calculated. Next, the width of the contour was multiplied by the height of the one, and the resulting value was assumed to be the size of the propagation shape of the strobe light. Figure 3 represent flow chart of these processes and Figs. 4~7 show the results.

Figs. 4&5 show processing (projection in the X-axis & Y-axis directions) results of the propagation shape image of the strobe light, shown in Fig. 2(a), respectively. We determined the threshold line to separate the effective propagation shape from the background properly, as shown in Figs. 4 & 5. The

threshold value for the segmentation process was calculated as follows.

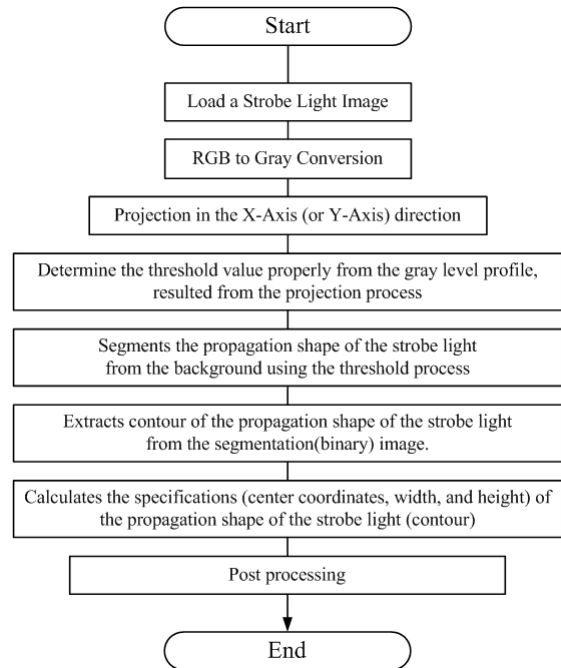


Figure 3. Image processing sequences for the analysis of a propagation shape of the strobe light

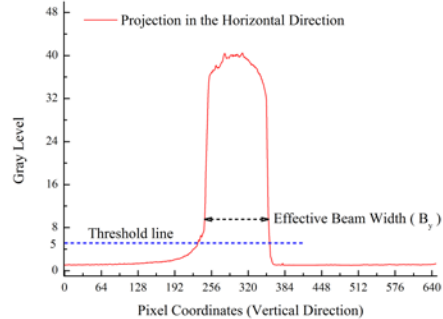


Figure 4. Gray level profile of a propagation shape of strobe light by the projection process (horizontal direction)

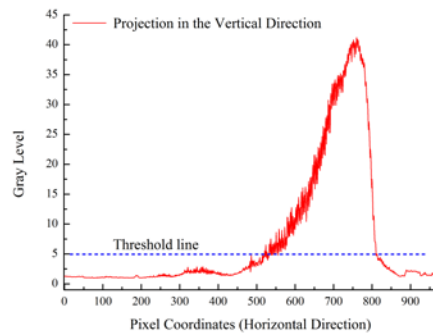


Figure 5. Gray level profile of a propagation shape of strobe light by the projection process (vertical direction)

$$I_{th} = I_{thresholdline} \times \frac{S_{vertical}}{B_Y} \quad (1)$$

In an equation (1),  $I_{th}$  is a threshold value for the segmentation process. And  $I_{thresholdline}$  is properly determined line (gray level) to separate effective propagation shape of the strobe light from background.  $S_{vertical}$  is a vertical dimension of the image, shown in Fig. 2 (a).  $B_Y$  is an effective beam width of the propagation shape of the strobe light in the vertical direction.

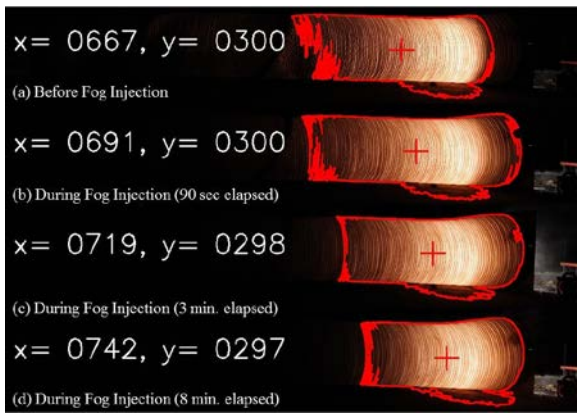


Figure 6. Contour of propagation shape of the strobe light.

Figure 6 show contours of the propagation shape of the strobe light images, shown in Figure 2. The x and y values displayed in the left-side of the Figure 6 are the center coordinates of the contour. The contours of the propagation shapes of the strobe lights, shown in Figs. 6(a)-(d), show that the length of the propagation shape of the strobe light in the horizontal direction increased at the early stage of fog injection (when the fog density was low), and decreased at the point of fog density saturation in the fog box (during the fog injection, approximately 8 min). This behavior is shown in Fig. 7.

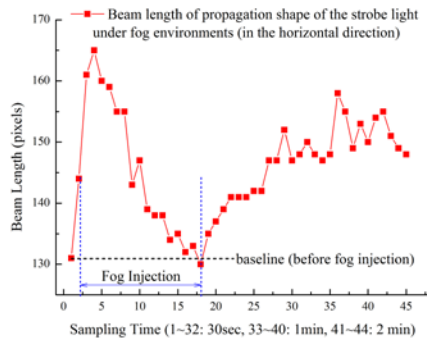


Figure 7. Beam length of the propagation shape of the strobe light inside the fog box.

From the Figure 7, we can see that when fog particles were injected into the fog box, the beam length of the propagation shape of the strobe light in the horizontal direction increased, except the 18th sampling point, shown in the X-axis of the Fig. 7, at which the beam length is below the baseline (before fog injection). However, the effective size of the beam propagation decreased because the center coordinates of the propagation shape of the strobe light, in the X-axis direction, were moved in the opposite direction of the beam propagation, as shown in Fig. 8.

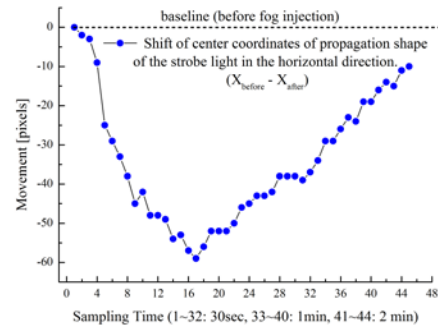


Figure 8. Movement of the center coordinates of the propagation shape of the strobe light.

The negative value (pixels) in the Y-axis of Fig. 8 means that the strobe light traveled in the reverse direction because a forward propagation of the strobe light was hindered by fog particles in the fog box. We designed simplified model to find the size of the backward propagation of the strobe light under dense fog environments in the fog box, as shown in Fig. 9.

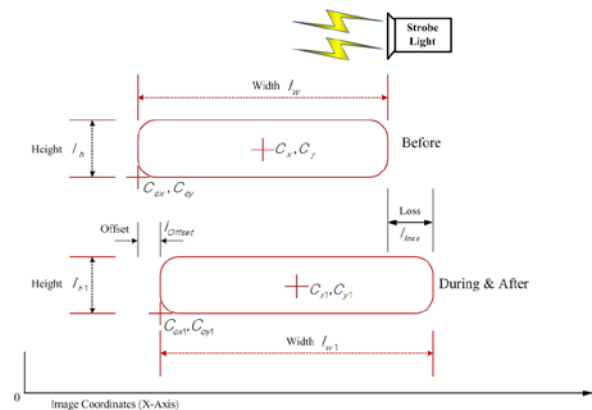


Figure 9. Simplified model of a beam propagation of the strobe light propagation

In Fig. 9, the upper contour (oval) model represents the beam propagation shape of the strobe light in the air before the fog injection. And the upper model is a simplified model of the images also, shown in Figs. 2(a) and 6(a). The lamp surface serves as a baseline of the propagation shape of the strobe light under fog

environments, shown on the top right side of the Fig. 9. The origin (0) at the bottom left of the image coordinate (X-axis), shown in the X-axis of Fig. 9, is supposed to be the arrival point of the strobe light beam. The lower contour (oval) model in Fig. 9 shows the beam propagation shape of the strobe light during or after fog injection. It is a simplified model of the images also, shown in Figs. 2(d) and 6(d).

In Fig. 9,  $I_{Offset}$  was calculated as follows.  $I_{Offset}$  is a size of the backward movement of the strobe light beam because it is reflected by the fog particles in the fog box.

$$I_{Offset} = C_{ox1} - C_{ox} \quad (2)$$

In Eq. (2),  $C_{ox1}$  represent an effective arrival distance of the strobe light beam during (or after) fog injection in the fog box, in the horizontal direction. And  $C_{ox}$  is an effective arrival range of the strobe light beam before fog injection. A lamp surface of the strobe light, shown in the top right side of Fig. 9, is the reference point for the effective arrival range of the strobe light beam. The effective arrival range of the strobe light beam can be expressed as follows:

$$C_{ox} = C_x - \frac{I_w}{2} \quad (3)$$

$$C_{ox1} = C_{x1} - \frac{I_{w1}}{2} \quad (4)$$

In Eq. (3),  $I_w$  indicates an effective arrival range (length) of the strobe light beam in the air before fog injection, and  $C_x$  is the center coordinate on the X axis of the propagation shape of the strobe light in the air before fog injection, as shown in the left side of Fig. 6 (a). In Eq. (4),  $I_{w1}$  indicates an effective arrival distance of the strobe light beam under dense fog environments where fog particles exist in the fog box. And  $C_{x1}$  is the center coordinate on the X axis of the propagation shape of the strobe light during (or after) fog injection in the fog box, as shown in the left side of Fig. 6(d).

Figure 10 shows a magnitude of the forward (when the fog density is low at the early stage of fog injection, 2nd ~ 4th sampling time) or backward movement of the strobe light beam, based on the calculation results of equation (2). From the Fig. 10, we can see that when the fog density was low in the fog box at the earlier stage of fog injection into the fog box (approximately within 2 min, 2nd ~ 4th sampling time), the strobe light beam was propagated far (about 12 pixels) in the distance than before the fog injection. When a fog concentration was almost saturated in the fog box at the 18th sampling

time, shown in Fig. 10, the strobe light beam was moved in the backward (about 56 pixels) direction.

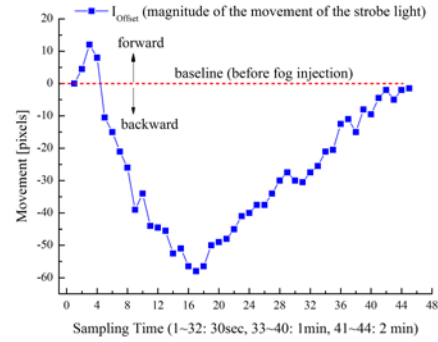


Figure 10. An effective propagation distance of the strobe light beam under fog environments

The propagation distance of the strobe light beam was decreased by about 43% at the time when the fog density was almost saturated, as follows.

$$\alpha = \frac{C_{ox\_18th\_frame} - C_{ox\_before}}{I_{w\_before}} \times 100\% \quad (5)$$

$$\alpha = \frac{680 - 623.5[pixels]}{13[pixels]} \times 100\% = 43.1\%$$

#### 4. Conclusions

We examined behaviors of the strobe light beam propagation in an aerosol-like non-visibility (dense fog) environment, which is a simulated visibility environments of the DBA (or severe accident) of the nuclear power plant. An image processing technique was used to estimate the propagation distance of the strobe light under dense fog environment. From the experimental and calculation results, we can see that the effective propagation distance of the strobe light was increased by about 9% from the time before fog injection when the fog density was low (at the early stage of fog injection). However, the effective propagation range of the strobe light beam was dropped significantly, by more than 43%, when the fog concentration was almost saturated in the fog box because most of the strobe light beam had been reflected and propagated in the backward direction, opposite to the lamp surface of the strobe light.

#### REFERENCES

- [1] Shikoku Electric Power Company, Incorporated, "Ikata Nuclear Power Plant Unit III, supplementary explanation data for additional installation of emergency station" pp 81-82, 2014.